Aggregation-Induced Long-Lived Phosphorescence in Non-Conjugated Polyurethane Derivatives at 77 K

Nan Jiang,[†,‖] Guang-Fu Li,[†,‖] Bao-Hua Zhang,[#] Dong-Xia Zhu,*[,†] Zhong-Min Su,*[,†] and Martin R. Bryce*[,§]

[†] Key Laboratory of Nanobiosensing and Nanobioanalysis at Universities of Jilin Province, Faculty of Chemistry, Northeast Normal University, Renmin Street No. 5268, Changchun 130024, P. R. China

[#] State Key Laboratory of Polymer Physics and Chemistry, Changchun Institute of Applied Chemistry, Chinese Academy of Sciences, Changchun 130022, P. R. China

[§] Department of Chemistry, Durham University, Durham DH1 3LE, UK

Supporting Information Placeholder

ABSTRACT: Achieving long persistent phosphorescence in polymers is a challenge even at low temperature. In this work, long persistent phosphorescence (> 1 s) is observed in non-conjugated polyurethane derivatives at 77 K, which is among the longest reported phosphorescent lifetimes for an organic polymer. The mechanism for this unusual behavior has been shown by steady-state photophysical characterization and time resolved emission spectra to arise from the formation of intra- and/or intermolecular carbonyl clusters at low temperature. The lifetime of long persistent phosphorescence is increased by the introduction of an aromatic monomer into the non-conjugated polyurethane chains. This is attributed to intra- and/or intermolecular n–π∗ transitions from electron rich carbonyl groups to the conjugated aromatic units thereby enhancing the intersystem crossing (ISC) rate. Coating an ultraviolet InGaAsN LED with a polyurethane derivative as the emitter gives cryogenic afterglow with long persistent phosphorescence which is observed for up to 7 s with naked eyes.

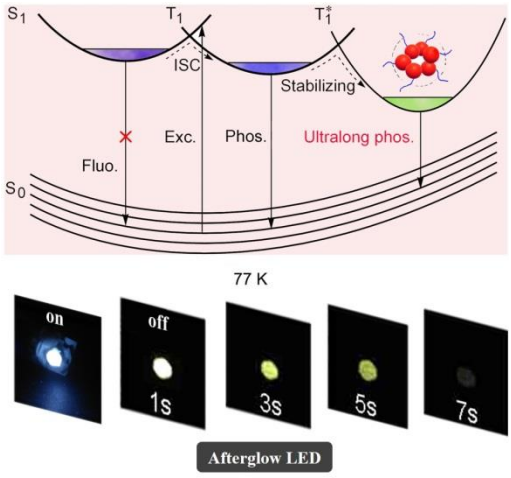

1. INTRODUCTION

Non-conjugated polymers are emerging as unconventional luminophores which do not possess typical polycyclic π-conjugated chromophoric units, and they have aroused great interest due to their significant academic value and promising technological applications.[1-5] Compared to the traditional organic luminescent materials, non-conjugated polymers show many advantages in terms of ease of chemical preparation, environmental-friendliness and applications in biological fluorescence imaging, due to their good hydrophilicity, chain flexibility and structural versatility.[6] Research in this area is still in its infancy, lacking clear guidelines for polymer design, and the mechanism of luminescence is not well understood. Generally, the presence of electron rich heteroatoms, such as nitrogen,[7-14] oxygen,[15-19] phosphorus,[20, 21] or sulfur,[22, 23] and/or unsaturated C=O,[24] C=C[25] and C≡N[26] subgroups into non-conjugated backbones is necessary for unconventional luminescence. Therefore, it is desirable to develop new types of luminescent non-conjugated polymers and to further probe the mechanism of emission in these systems.

Polyurethanes (PUs) are industrial-scale non-conjugated polymers with many desirable properties, such as facile synthesis, good mechanical toughness, abrasion resistance and low-temperature resistance. They have found broad applications as shape-memory materials, building insulation, components of furniture and fabrics in our daily life.[27-29] However, their luminescent properties and optoelectronic applications are largely unexplored.[30-33] We hypothesized that by virtue of the structural flexibility and electron rich heteroatoms (O and N) non-conjugated polyurethanes could possess interesting photophysical properties due to the following considerations. First, the non-conjugated architecture may effectively avoid aggregation-induced quenching of emission which is facilitated by strong π-π stacking interactions in conjugated materials. Consequently efficient emission could occur at high concentrations. Second, the non-conjugated PU structure blocks strong electronic coupling, and is therefore favorable for blue emission. Third, due to the good mechanical flexibility of PUs, the individual polymer chains are in close proximity. Excited state charge transfer processes may, therefore, readily occur through intermolecular interactions, leading to a small singlet–triplet splitting (ΔE_{ST}) which, in turn, could promote intersystem crossing (ISC) as well as reverse ISC (RISC)[34] between singlet (S_1) and triplet (T_1) states, thus prolonging the exciton lifetimes.

In this work, a series of three non-conjugated polyurethanes **PU1**–**PU3** have been rationally designed: **PU1** incorporates the classical π-aromatic binaphthyl chromophores, whereas **PU2** and **PU3** have π-aromatic biphenyl chromophores and non-aromatic units, respectively, in the polymer backbones. **PU1**–**PU3** all show unusually long persistent luminescence (LPL) at 77 K - including **PU3** with no aromatic backbone units. There is an increase in luminescent lifetimes with the introduction of aromatic monomer units, indicating that the LPL lifetimes can be rationally tuned by the incorporation of aromatic chromophores into these PU derivatives. Thus, among the three PUs, **PU1**, exhibits the longest phosphorescent decay times of 1.4 s and 0.52 s in solution and powder states, respectively.. Steady-state photophysical data and time resolved emission spectra (TRES) lead to the conclusion that the formation

of intra- and/or intermolecular carbonyl clusters at low temperature plays a key role in obtaining long persistent phosphorescence. These results, therefore, establish that polyurethane derivatives can be designed to display aggregation-induced persistent phosphorescence. Furthermore, benefiting from the excellent LPL at high concentration for **PU1**, a cryogenic afterglow InGaAsN light-emitting diode (LED) has been fabricated using **PU1** as the emitter. Long persistent phosphorescence is observed for up to 7 s by naked eyes.

2. RESULTS AND DISCUSSION

Synthesis. The PUs were synthesized by dissolving polyethylene glycol mono-methyl ether (M_w 200 g mol^{-1}, 0.396 g, 1.98 mmol) and either (*R*)-1-(2-hydroxynaphthalen-1-yl)naphthalen-2-ol ((*R*)-BINOL) (2.62 mmol), or 2,2'-biphenol (2.62 mmol), or 1,2-ethanediol (2.62 mmol) in anhydrous THF (10 mL). Hexamethylene diisocyanate (0.608 g, 3.61 mmol) and 1,4-diazabicyclooctane triethylenediamine (DABCO) (12 mg, 0.06 mmol) were then added to the reaction mixture which was stirred at 75 ºC for 7 h under N_2 until the clear solution became viscous, indicating polymerization had occurred. After cooling to room temperature, excess diethyl ether was added to precipitate the products **PU1** (M_n = 3118 g mol^{-1}), **PU2** (M_n = 1845 g mol^{-1}) and **PU3** (M_n = 3544 g mol^{-1}), respectively, with yields >60% (Scheme 1). The detailed synthetic methods and ^{1}H NMR and FTIR spectroscopic characterization are given in the experimental section and supporting information.

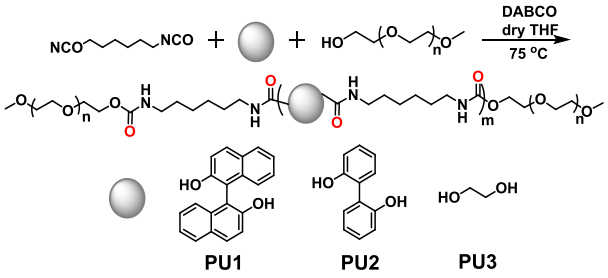

Scheme 1. Synthetic routes for **PU1**, **PU2** and **PU3**.

Physical Properties. Most aggregation-induced emission (AIE) materials are almost non-emissive in both dilute and highly concentrated solutions, whereas bright emission can be observed in the solid and host-guest doped film states due to the restriction of intramolecular motion (RIM).[35] At room temperature, **PU1**–**PU3** show faint emission in dilute solution, whereas intense emission is observed in highly concentrated solution and in the solid states, which is atypical AIE behavior. The absorption spectra of **PU1** in different ratios of acetone–water mixtures are depicted in Figure S5a. The major absorption peak at 339 nm is assigned to the R band of an n→π* transition, suggesting that O, and/or N atoms are conjugated with aromatic rings in the system.[36] The progressively enhanced absorption intensity with an extended red edge for increased water% is evidence for the formation of nano-aggregates, which was further established by transmission electron microscopy (TEM) results. The TEM image of **PU1** showed dispersed nanoparticles with a diameter in the range of 20–50 nm in dilute acetone solution (1×10^{-5} M) (Figure S6a). However, when the add-

ed water fraction reached 90%, irregularly shaped (chains and particles) larger aggregates were formed (Figure S6d). This indicates that nano-aggregation is enhanced by the addition of water which is a poor solvent.

The corresponding emission spectra of **PU1** in different ratios of acetone–water mixtures are shown in Figure 1a. **PU1** exhibits faint emission in dilute acetone solution (10^{-5} M), which is considerably increased when the water fraction exceeds ca. 60%. Emission peaks at 373, 410, 447, 479, 513 and 561 nm with different lifetimes (τ) of 1.1, 1.24, 6.32, 6.7 and 6.64 ns are observed. Meanwhile, the emission spectrum of monomer (*R*)-BINOL was also measured in both the solution and powder states (Figure S7) and only UV emission with a peak at 370 nm was observed. This indicates that the emission peak at 373 nm in **PU1** originates from the excited state of the (R)-BINOL unit. The other emission peaks of **PU1** are indicative of the presence of different emissive species in solution, derived from various aggregated structures owing to chain folding and aggregation.[26] When the water fraction increases up to 90%, 100-fold increase in emission intensity of **PU1** was observed in comparison with the pure acetone solution. The photoluminescence quantum yield (PLQY) of **PU1** is 21%. All the above photophysical results demonstrate that **PU1** displays AIE.

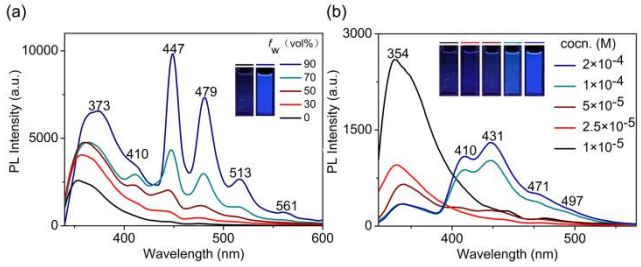

Figure 1. (a) Emission spectra of **PU1** (1×10^{-5} M) in acetone–water mixtures with different water fractions (0–90% v/v) at room temperature. Inset: photographs of **PU1** (M_n 3118 g mol^{-1}) in pure acetone solution and acetone–water mixture (f_w = 90%) under 365 nm UV illumination. **(b)** PL spectra of **PU1**/acetone with different concentrations. Inset: photographs taken under 365 nm UV light.

In contrast to the typical AIE effect,[35] a concentration dependent emission behavior was observed for **PU1** in acetone solution (Figure 1b). The concentrations of **PU1** were selected within the range of 1×10^{-5} M – 2×10^{-4} M. The emission intensity of **PU1** increases when the concentration increased to 1×10^{-4} M and shows similar emission features to the acetone/water mixtures at low concentration of 1×10^{-5} M. Meanwhile, the similar features in the UV-vis absorption spectra of **PU1** in acetone (Figure S5b) to the acetone–water mixtures (Figure S5a) demonstrate that the aggregates form in both conditions. TEM reveals that the sizes of nanoparticles increased from ca. 20 nm to ca. 200 nm with an incremental increase in concentration (10^{-5} M – 2×10^{-4} M) of **PU1** (Figures S6a-c). To investigate the possible influence of hydrogen bonding interactions in the aggregated state, ^{1}H NMR spectra were recorded for concentrations of 2.5 mg mL^{-1} and 5 mg mL^{-1} of **PU1** in DMSO-d_6. The almost identical ^{1}H NMR spectra for both solutions (Figure S8) with no N-H shift, implies that hydrogen bonding interactions are absent or very weak in the aggregated state.[37] Thus, it is rational to ascribe the AIE mechanism of **PU1** to the formation of carbonyl clusters.[6, 24] As illustrated in Figure 2,

the linear **PU1** chains will be extended in dilute solution, effectively isolating the carbonyl groups and, therefore, leading to only faint emission (Figure 2a). In concentrated solution or the aggregated state, **PU1** chains will entangle and approach each other in close proximity to form carbonyl clusters, affording through-space electronic overlap between lone pairs and π electrons (Figures 2b and 2c). Consequently, in the more rigidified conformations there is enhanced electronic conjugation, which, in turn, leads to enhanced emission. In previous work the unconventional emission in non-conjugated linear and hyperbranched polymers, e.g. siloxane-poly(amidoamine) dendrimers, was explained by aggregation of multiple carbonyl groups.[6,24] LPL of non-conjugated polyacrylonitrile, without any aromatic chromophore in the molecule, has been ascribed to clustering of the pendant cyano groups in concentrated solution and solid samples affording through-space electronic communication.[26]

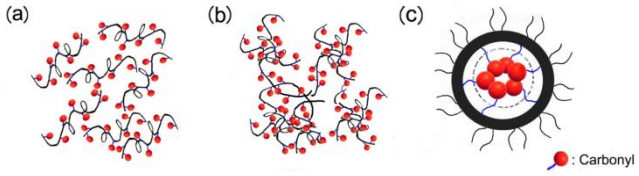

Figure 2. Schematic illustration of **PU1** (a) dilute solution, (b) concentrated solution, and (c) carbonyl clusters in the aggregated state.

The emission spectra of **PU1** in the powder state were explored at different excitation wavelengths (Figure S9). Under UV illumination powder **PU1** exhibits bright emission covering the UV and visible regions. The weak lower energy emission peaks are consistent with those observed in high concentration acetone solution and acetone/water mixtures (Figure 1a), indicating the presence of various emissive species that might be derived from different carbonyl clusters. The semicrystallinity of **PU1** shown by powder X-ray diffraction (Figure S10) offers additional physical restraints and is favourable for light emission.[26]

Cryogenic long persistent phosphorescence. The photophysical properties of **PU1** were further studied at 77 K in dilute 2-methylTHF solution (10^{-5} M). As shown in Figure 3a, upon irradiation with UV light at 365 nm, the steady-state emission spectra showed multiple profiles with major peaks at 409, 437, 463 and 497 nm, which is similar to the behavior at room temperature (Figure 1b). Upon removal of the ultraviolet irradiation, LPL lasting for 2 s with changed emission color was clearly observed by naked eyes (Figure 3a insert images and Supplementary Movie 1). Thus **PU1** exhibits LPL which is rarely observed in a non-conjugated polymer.[38-41] The resistance of the low temperature phosphorescence to photobleaching was further confirmed by 20 repeated excitation cycles with high reproducibility (Figure S11). To further investigate this rare LPL, transition-state emission spectra (TRES) were obtained. As shown in Figure 3a, the TRES of **PU1** showed multiple emission profiles with major peaks at 445, 490, 513 and 560 nm. Decay times corresponding to emission peaks were measured individually. Interestingly, in contrast to the fast fluorescent emission ($S_1 \rightarrow S_0$) with lifetimes of a few nanoseconds at room temperature, long persistent phosphorescent (T_1) lifetimes beyond a

few hundred milliseconds were observed in each peak (Table S1). The longest luminescent lifetime of 1.4 s was observed in the 560 nm peak (Figure 3b). For comparison, a lifetime of 1.2 s has been reported at room temperature for poly(methyl methacrylate) (PMMA) with an *N*-substituted naphthalimide end group.[42] Poly(lactic acid) functionalized with difluoroboron dibenzoylmethane has a lifetime of 1.75 s at 77 K.[43] Thus, the T_1 excited state with long decay times dominates the emission behavior of **PU1** at 77 K. It is known that at low temperature, the rates of internal conversion (IC), intersystem crossing (ISC), and collisional quenching are commonly restricted due to the rigidity of the frozen sample, resulting in phosphorescence with microsecond (μs) decay times.[44] However, to the best of our knowledge, such long persistent phosphorescence (~0.8 s) has not been previously reported in an organic polymer at 77 K at a concentration as low as 10^{-5} M (Table S1).

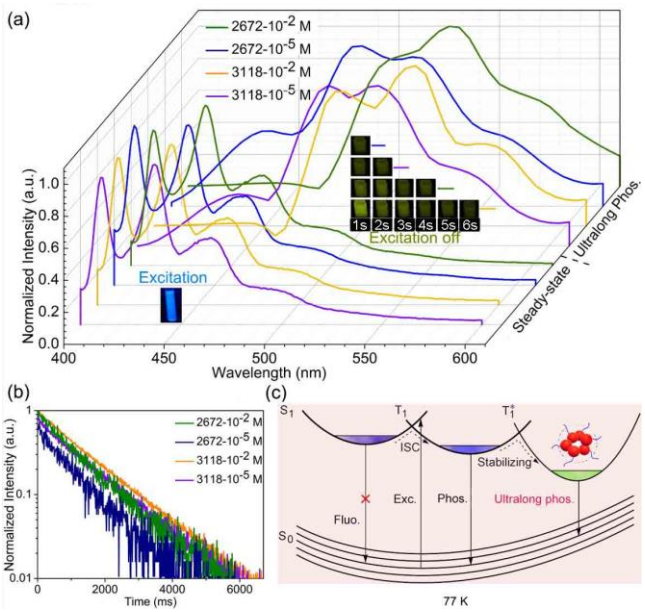

Figure 3. (a) The steady-state photoluminescence and long phosphorescence spectra of **PU1** with different average molecular weights (M_n 2672 or 3118 g mol^{-1}), and different concentrations in 2-MeTHF solutions at 77 K. Insets show the corresponding photographs taken at different times before and after turn-off of the excitation (365 nm) at 77 K. (b) Phosphorescence decays at 560 nm of **PU1** in 2-MeTHF solution. (c) The proposed LPL mechanism for **PU1** at 77 K.

What is the reason for this unusual LPL phenomenon? Based on the formation of nanoparticles at low concentration (10^{-5} M) of **PU1**, as observed from the TEM image (Figure S6a), we propose that the electron rich heteroatoms and the good flexibility in the polyurethane chains promote the formation of clusters through intra- and/or intermolecular interactions even at this low concentration. This is a different situation from pure small organic molecules that are regarded as isolated molecules without any intra- or intermolecular interactions in dilute solution.[45] The spacial electronic overlap between lone pairs and π electrons within the carbonyl clusters in **PU1** explains the fascinating cryogenic long persistent phosphorescence. To validate our hypothesis, PMMA matrices doped with **PU1** (2%) were used in solid-state "dilution" experiments to probe the role of intramolecular motions on the observa-

tion of LPL. In contrast to the long phosphorescent lifetime (~0.8 s) observed in the low concentration solutions of pure **PU1** at 77 K, a PMMA doped film exhibited a short fluorescent lifetime of 2 ns (Figure S12). This confirms that effectively restricting intramolecular motions is not the reason for the observed LPL of **PU1** at 77 K.

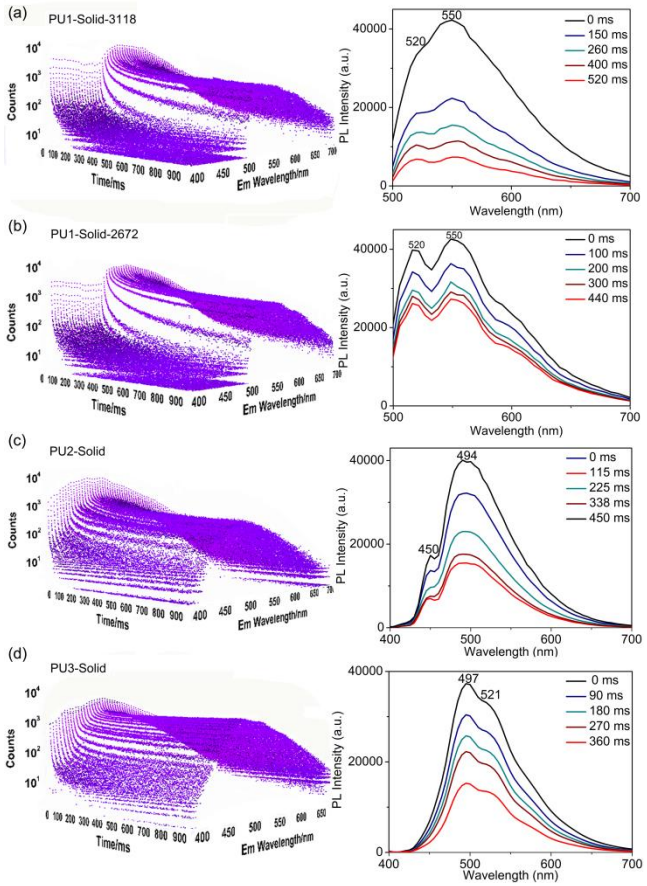

Figure 4. 3D time resolved emission spectra (TRES) (left) and corresponding transition-state emission spectra (right) of **PU1**–**PU3** in powder state at 77 K.

More detailed photophysical measurements certify that carbonyl clusters plays a key role in obtaining LPL. Concentration dependent emission data in 2-MeTHF solution are shown in Figure 3b and Table S1. Persistent phosphorescence with λ_{max} at 560 nm was selected, and the decay time of **PU1** increased from 0.76 s to 1.44 s upon increasing the concentration from 10^{-5} to 10^{-2} M. This concentration-promoted LPL is consistent with the formation of clusters. Furthermore, the influence of different degrees of polymerization in **PU1** on LPL was also considered by comparing samples with M_n 3118 and 2672 g mol^{-1}. The two samples showed similar concentration dependent LPL (Figure 3b and Table S1). It is worth noting that the decay lifetime increases significantly with the increased degree of polymerization (Figure 3b and Table S1). This can be attributed to increased formation of clusters by the more flexible chains and the electron rich heteroatoms of **PU1** (3118 g mol^{-1}). In contrast to the long phosphorescent lifetime (~0.8 s) observed for **PU1** at 77 K, (*R*)-BINOL exhibited a short phosphorescent lifetime of 8.77 μs in dilute 2-MeTHF

soluition (Figure S13). Therefore, all the above results provide substantial evidence that aggregation induced by carbonyl clusters is a key requisite for LPL at 77 K in **PU1**.

In the powder state of **PU1**, LPL is also observed for both molecular weight samples (M_n 3118 and 2672 g mol^{-1}) at 77 K. The transition-state emission spectra of **PU1** show a broad emission band with peaks at 520 and 550 nm (Figures 4a, 4b). LPL behavior of **PU1** (3118 g mol^{-1}) was observed by naked eyes for a period of 4 s, and the corresponding decay time was 0.52 s. Similar to the solution state, an increased decay time was observed from the lower molecular weight (2672 g mol^{-1}, 0.44 s) compared to the higher molecular weight (3118 g mol^{-1}, 0.52 s) of powder samples of **PU1** (Figure S15 and Table S2, λ_{max} 550 nm). The lifetime data for **PU1** (M_n 2672 g mol^{-1}) in the pristine film state at two different concentrations of 10 mg and 100 mg were also investigated at 77 K. There is an increase in luminescence lifetime with increasing concentration of **PU1** (Table S3).

To further probe the LPL mechanism of **PU1**, the S_1 and T_1 energy levels were estimated from the onset wavelengths of the 298 K and 77 K steady-state emission spectra (Figure S16), respectively, measured in solution. The small S_1-T_1 energy gap (ΔE_{ST} 0.06 eV) could promote the ISC as well as reverse ISC (RISC) processes, thus prolonging the excited state lifetimes.[34] At room temperature, fast fluorescence from the S_1 state with a lifetime of a few nanoseconds is observed due to the spin-forbidden T_1 state. Meanwhile, thermally activated delayed fluorescence (TADF) was not observed, perhaps due to a lack of spin-vibronic coupling.[46] At 77 K, assisted by the low temperature, the singlet excitons were rapidly converted to triplet excitons through a fast ISC process, and bright blue phosphorescence was observed in steady-state conditions, and the corresponding T_1 energy level was calculated as 3.09 eV (Figure S16). On removal of the ultraviolet irradiation, the emission color changed from blue to green-yellow with a lower energy level of 2.71 eV (Figure S16). This result is evidence for the existence of a stabilized excited state (T_1^*) which functions as an energy trap, and maybe delocalized on several neighbouring polyurethane chains,[47] resulting in long phosphorescence by facilitating radiative pathways and suppressing non-radiative deactivation decays. The proposed LPL mechanism of **PU1** is shown in Figure 3c.

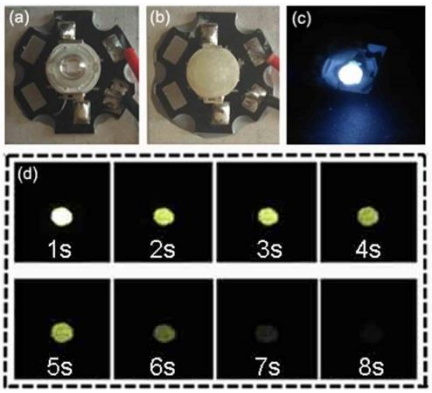

Figure 5. (a) An emitting 3 mm diameter reference ultraviolet InGaAsN LED (λ_{em} = 395 nm). (b) The same LED coated with a thin layer of 3.5 wt% **PU1** (not turned on). (c) The coated LED was turned on immediately after it was removed from liquid nitrogen and emits bright blue emission. (d) The phosphorescence images taken at 1 s intervals after turning off the operating voltage.

Intermolecular n–π* transitions from electron-rich heteroatoms to conjugated (hetero)aromatic units in small molecules have been shown by the groups of Chi,[48] Li,[49] Huang[50] and Tang[51-53] to facilitate ISC leading to LPL behavior. Recently Li et al. reported that intermolecular π–π interactions play an important role in persistent phosphorescence.[54-56] Therefore, it is rational to check the role of the aromatic unit in obtaining LPL in our polyurethane system. For comparison with **PU1**, analogs were prepared with a smaller biphenyl unit (**PU2**, M_n = 1845 g mol^{-1}) and with a saturated unit (**PU3**, M_n = 3544 g mol^{-1}), replacing the binaphthyl unit of **PU1**. The luminescence decays of **PU2** and **PU3** were measured in the powder state at 77 K. As shown in Figures 4c, 4d and Table S2, both **PU2** and **PU3** exhibit LPL behavior, demonstrating that the aromatic unit is not essential for LPL in polyurethane derivatives. Nonetheless, the decay times clearly increase with the introduction of aromatic units into the non-conjugated PU chains (Table S2), revealing that the intra- or intermolecular n–π* transition from electron rich carbonyl groups to the conjugated aromatic units is favorable for enhancing LPL behavior.

Cryogenic afterglow LED. To investigate the potential optoelectronic applications of the polyurethane materials, a cryogenic afterglow LED was fabricated by adding dropwise a solution of **PU1** (M_n 2672 g mol^{-1}) in 2-methylTHF onto an ultraviolet InGaAsN LED chip (λ_{em} = 395 nm). As shown in Figure 5b, due to the favorable viscosity of the polymer, **PU1** (50 mg) uniformly adheres to the surface of the LED to form a thin film. Immediately after removing the LED bulb from the 77 K environment, upon electrical excitation with a low voltage (3 V) bright blue emission was obtained (Figure 5c). When the applied voltage was turned off, green persistent emission is observed for as long as 7 s, attributed to the phosphorescence of **PU1** (Figure 5d and Supplementary Movie 2).

3. CONCLUSION

In summary, visible long-lived luminescence (> 1 s) in a non-conjugated polyurethane system at 77 K has been reported for the first time. The aggregation-induced LPL mechanism was shown by detailed photophysical and time resolved emission spectra to arise from spacial electronic overlap between lone pairs and π electrons through the formation of carbonyl clusters. The introduction of conjugated aromatic units into the backbone of the non-conjugated polymer chains has been shown to promote the ISC process through intra- or intermolecular n–π* transitions and further increase the decay times of LPL. Furthermore, benefiting from the excellent aggregation-induced LPL, a cryogenic afterglow light-emitting diode (LED) has been fabricated and persistent phosphorescence has been observed for up to 7 s by naked eyes. This work should promote new studies on the rational design of non-conjugated polymers which display aggregation-induced long-lived luminescence, leading to further applications in optoelectronic

technologies. In the future, unconventional ultralong-lived luminescence may be realized by tailoring the structure of a non-conjugated polymer.

4. EXPERIMENTAL SECTION

Synthesis. PU1 was prepared according to the following general procedure: A mixture of (*R*)-BINOL (0.750 g, 2.62 mmol), poly-ethylene glycol mono-methyl ether (M_w = 200 g mol^{-1}; 0.396 g, 1.98 mmol), anhydrous THF (10 mL)， hexam-ethylene di-isocyanate (0.608 g, 3.61 mmol) and DABCO (12 mg, 0.105 mmol) was heated at 75°C for 7 h under a nitrogen atmosphere until the clear solution became significantly viscous, indicating polymerization. After cooling to room temperature, the mixture was pre-cipitated from excess diethyl ether. Then the product was dried under vacuum at room temperature for 24 h to obtain the resulting polymer Yield: 61%. ^{1}H NMR (500 MHz, DMSO-d_6, δ [ppm]): 7.01-8.08 (broad, 12H; (*R*)-BINOL protons), 4.04 (s, 4H), 3.37-3.58 (broad, PEG protons), 3.32 (s, 6H; PEG terminal -OCH_3 protons), 2.63-2.98 (broad, 4H), 1.09 (broad, 4H), 0.75 (broad, 4H). FTIR: 3339 cm^{-1}(N-H), 2860 and 2941cm^{-1} (-CH_2- asymmetric and symmetric stretch), 1692 (C=O), 1113 cm^{-1} (C-O-C stretch PEG). Anal. Calcd for $C_{46}H_{62}N_4O_{11}$: C, 65.24; H, 7.33; N, 6.62. Found: C, 65.38; H, 7.16; N, 6.16. M_n = 3118 g mol^{-1}, PDI = 1.52.

The synthetic procedure for **PU2** was the same as **PU1**, except monomer 2,2'-biphenol (0.488 g, 2.62 mmol) was used instead of (*R*)-BINOL. Yield: 63%. ^{1}H NMR (500 MHz, DMSO-d_6, δ [ppm]): 7.02-7.44 (broad, 8H; 2,2'-biphenol protons), 4.03 (s, 4H), 3.40-3.60 (broad, PEG protons), 3.32 (s, 6H; PEG terminal -OCH_3 protons), 2.88 (broad, 4H), 1.16 (broad, 4H), 1.32 (broad, 4H). FTIR: 3327 cm^{-1}(N-H), 2858 and 2933 cm^{-1} (-CH_2-asymmetric and symmetric stretching), 1715 cm^{-1} (C=O), 1111 cm^{-1} (C-O-C stretching PEG). Anal. Calcd for $C_{38}H_{58}N_4O_{11}$: C, 61.13; H, 7.77; N, 7.51. Found: C, 61.38; H, 7.16; N, 8.16. M_n = 1845 g mol^{-1}, PDI = 1.16.

The synthetic procedure of **PU3** was the same as **PU1**, except monomer 1,2-ethanediol (0.163 g, 2.62 mmol) was used instead of (R)-BINOL. Yield: 64%.^{1}H NMR (500 MHz, DMSO-d_6, δ [ppm]): 7.16 (s, 2H), 4.06 (broad, 4H), 3.93 (broad, 4H), 3.41-3.58 (broad, PEG protons), 3.32 (s, 6H; PEG terminal -OCH_3- protons), 2.94 (s, 4H), 1.35 (s, 4H),1.22 (s, 4H). FTIR: 3326 cm^{-1} (N-H), 2862 and 2939 cm^{-1} (-CH_2- asymmetric and symmetric stretching), 1684 cm^{-1} (C=O), 1144 cm^{-1} (C-O-C stretching PEG). Anal. Calcd for $C_{36}H_{54}N_4O_{11}$: C, 60.17; H, 7.52; N, 7.80; O, 24.51. Found: C, 60.38; H, 7.46; N, 7.86; O, 24.30. The M_n of **PU3** is 3544 g mol^{-1} calculated from the ^{1}H NMR spectra.

Photophysical Characterization. UV-vis absorption spectra were recorded on a Shimadzu UV-3100 spectrophotometer. Steady-state emission spectra, the excited-state lifetimes (τ), photoluminescence quantum yields (Φ_p) and time resolved emission spectra (TRES) were recorded on an Edinburgh FLS-920 spectrofluorimeter equipped with a xenon arc lamp (Xe900), a nanosecond hydrogen flash-lamp (nF920) and a microsecond flash-lamp (μF900), respectively. For fluorescence decay measurements, subnano-second optical pulses over the VUV-to-NIR spectral range were provided using a hydrogen flash lamp. The microsecond flash lamp

produces short, typically a few μs, and high irradiance optical pulses for phosphorescence decay measurements in the range from microseconds to seconds. The lifetimes (τ) of the luminescence were obtained by fitting the decay curve with a multi-exponential decay function where

$$I(t) = \sum_i A_i e^{-\frac{t}{\tau_i}}$$

A_i and τ_i represent the amplitudes and lifetimes, respectively, of the individual components for multi-exponential decay profiles.

Fabrication of cryogenic afterglow LED. A cryogenic afterglow light-emitting diode (LED) was fabricated by dropwise addition of a solution of **PU1** (M_n 2672 g mol^{-1}, 50 mg, 3.5 wt%) in 2-methylTHF on an ultraviolet InGaAsN LED chip (λ_{em} 395 nm) at room temperature. The photographs and supporting movies were recorded with a cellphone (HUAWEI Nova 1).

ASSOCIATED CONTENT

Supporting Information

The Supporting Information is available free of charge on the ACS Publications website at DOI: xxxxx.

Additional structural characterization; copies of NMR and FTIR spectra; additional photophysical data; transmission electron microscopy (TEM) data; movies showing persistent emission.

AUTHOR INFORMATION

Corresponding Authors

*zhudx047@nenu.edu.cn

*zmsu@nenu.edu.cn

*m.r.bryce@durham.ac.uk

Author Contributions

‖ Nan Jiang and Guang-Fu Li contributed equally.

Notes

The authors declare no competing financial interest.

ACKNOWLEDGMENT

The work was funded by NSFC (No.51473028), the key scientific and technological project of Jilin province (20150204011GX, 20160307016GX), the Development and Reform Commission of Jilin province (20160058). M.R.B. thanks EPSRC grant EL/L02621X/1 for funding.

REFERENCES

(1) Mei, J.; Leung, N. L.; Kwok, R. T.; Lam, J. W.; Tang, B. Z. Aggregation-Induced Emission: Together We Shine, United We Soar! *Chem. Rev.* **2015**, *115*, 11718–11940.

(2) Zhang Yuan, W.; Zhang, Y. Nonconventional macromolecular luminogens with aggregation-induced emission characteristics. *J. Polym. Sci. Pol. Chem.* **2017**, *55*, 560–574.

(3) Restani, R. B.; Morgado, P. I.; Ribeiro, M. P.; Correia, I. J.; Aguiar-Ricardo, A.; Bonifacio, V. D. Biocompatible Polyurea Dendrimers with pH-Dependent Fluorescence. *Angew. Chem. Int. Ed.* **2012**, *51*, 5162–5165.

(4) Sun, M.; Hong, C. Y.; Pan, C. Y. A unique aliphatic tertiary amine chromophore: fluorescence, polymer structure, and application in cell imaging. *J. Am. Chem. Soc.* **2012**, *134*, 20581–20584.

(5) Zhu, S.; Song, Y.; Shao, J.; Zhao, X.; Yang, B. Non-Conjugated Polymer Dots with Crosslink-Enhanced Emission in the Absence of Fluorophore Units. *Angew. Chem. Int. Ed.* **2015**, *54*, 14626–14637.

(6) Huang, T.; Wang, Z.; Qin, A.; Sun, J.; Tang, B. Luminescent polymers containing unconventional chromophores. *Acta Chim. Sinica* **2013**, *71*, 979–990.

(7) Lee, W. I.; Bae, Y.; Bard, A. J. Strong blue photoluminescence and ECL from OH-terminated PAMAM dendrimers in the absence of gold nanoparticles. *J. Am. Chem. Soc.* **2004**, *126*, 8358–8359.

(8) Wang, D. J.; Imae, T. Fluorescence emission from dendrimers and its pH dependence. *J. Am. Chem. Soc.***2004**, *126*, 13204–13205.

(9) Wu, D. C.; Liu, Y.; He, C. B.; Goh, S. H. Blue Photoluminescence from Hyperbranched Poly(amino ester)s. *Macromolecules* **2005**, *38*, 9906–9909.

(10) Chu, C. C.; Imae, T. Fluorescence Investigations of Oxygen-Doped Simple Amine Compared with Fluorescent PAMAM Dendrimer. *Macromol. Rapid. Comm.* **2009**, *30*, 89–93.

(11) Lin, S. Y.; Wu, T. H.; Jao, Y. C.; Liu, C. P.; Lin, H. Y.; Lo, L. W.; Yang, C. S. Unraveling the Photoluminescence Puzzle of PAMAM Dendrimers. *J. Phys. Org. Chem.* **2011**, *17*, 7158–7161.

(12) Pastor, P. L.; Chen, Y.; Shen, Z.; Lahoz, A.; Stiriba, S. E. Unprecedented Blue Intrinsic Photoluminescence from Hyperbranched and Linear Polyethylenimines: Polymer Architectures and pH-Effects. *Macromol. Rapid Comm.* **2007**, *28*, 1404–1409.

(13) Wang, R. B.; Yuan, W. Z.; Zhu, X. Y. Aggregation-induced emission of non-conjugated poly(amido amine)s: discovering, luminescent mechanism understanding and bioapplication. *Chinese. J. Polym. Sci.* **2015**, *33*, 680–687.

(14) Yu, W.; Wu, Y.; Chen, J.; Duan, X.; Jiang, X. F.; Qiu, X.; Li, Y. Sulfonated ethylenediamine–acetone–formaldehyde condensate: preparation, unconventional photoluminescence and aggregation enhanced emission. *RSC Adv.* **2016**, *6*, 51257–51263.

(15) Gong, Y.; Tan, Y.; Mei, J.; Zhang, Y.; Yuan, W.; Zhang, Y.; Sun, J.; Tang, B. Z. Room temperature phosphorescence from natural products: Crystallization matters. *Sci. China Chem.* **2013**, *56*, 1178–1182.

(16) Niu, S.; Yan, H.; Chen, Z.; Yuan, L.; Liu, T.; Liu, C. Water-Soluble Blue Fluorescence-Emitting Hyperbranched Polysiloxanes Simultaneously Containing Hydroxyl and Primary Amine Groups. *Macromol. Rapid Comm.* **2016**, *37*, 136–142.

(17) Pucci, A.; Rausa, R.; Ciardelli, F. Aggregation-Induced Luminescence of Polyisobutene Succinic Anhydrides and Imides. *Macromol. Chem. Phys.* **2008**, *209*, 900–906.

(18) Yu, W.; Wang, Z.; Yang, D.; Ouyang, X.; Qiu, X.; Li, Y. Nonconventional photoluminescence from sulfonated acetone–formaldehyde condensate with aggregation-enhanced emission. *RSC Adv.* **2016**, *6*, 47632–47636.

(19) Zhao, E.; Lam, J. W. Y.; Meng, L.; Hong, Y.; Deng, H.; Bai, G.; Huang, X.; Hao, J.; Tang, B. Z. Poly[(maleic anhydride)-*alt*-(vinyl acetate)]: A Pure Oxygenic Nonconjugated Macromolecule with Strong Light Emission and Solvatochromic Effect. *Macromolecules* **2014**, *48*, 64–71.

(20) Bhattacharya, S.; Rao, V. N.; Sarkar, S.; Shunmugam, R. Unusual emission from norbornene derived phosphonate molecule–a sensor for Fe^{III} in aqueous environment. *Nanoscale* **2012**, *4*, 6962–6966.

(21) Liu, T.; Meng, Y.; Wang, X.; Wang, H.; Li, X. Unusual strong fluorescence of a hyperbranched phosphate: discovery and explanations. *RSC Adv.* **2013**, *3*, 8269–8275.

(22) Li, W.; Wu, X.; Zhao, Z.; Qin, A.; Hu, R.; Tang, B. Z. Catalyst-free, atom-economic, multicomponent polymerizations of aromatic diynes, elemental sulfur, and aliphatic diamines toward luminescent polythioamides. *Macromolecules* **2015**, *48*, 7747–7754.

(23) Yan, J.; Zheng, B.; Pan, D.; Yang, R.; Xu, Y.; Wang, L.; Yang, M. Unexpected fluorescence from polymers containing dithio/amino-succinimides. *Poly. Chem.* **2015**, *6*, 6133–6139.

(24) Lu, H.; Feng, L.; Li, S.; Zhang, J.; Lu, H.; Feng, S. Unexpected Strong Blue Photoluminescence Produced from the Aggregation of Unconventional Chromophores in Novel Siloxane–Poly(amidoamine) Dendrimers. *Macromolecules* **2015**, *48*, 476–482.

(25) Yang, L.; Wang, L.; Cui, C.; Lei, J.; Zhang, J. Stöber strategy for synthesizing multifluorescent organosilica nanocrystals. *Chem. Commun.* **2016**, *52*, 6154–6157.

(26) Zhou, Q.; Cao, B.; Zhu, C.; Xu, S.; Gong, Y.; Yuan, W. Z.; Zhang, Y. Clustering-Triggered Emission of Nonconjugated Polyacrylonitrile. *Small* **2016**, *12*, 6586–6592.

(27) Lendlein, A. Kelch, S. Shape-memory polymers. *Angew. Chem. Int. Ed.* **2002**, *41*, 2034–2057.

(28) Chattopadhyay, D. K.; Raju, K. V. S. N. Structural engineering of polyurethane coatings for high performance applications. *Prog. Poly. Sci.* **2007**, *32*, 352–418.

(29) Liu, C.; Qin, H.; Mather, P. T. Review of progress in shape-memory polymers. *J. Mater. Chem.* **2007**, *17*, 1543–1558.

(30) Fan, Z. X.; Zhao, Q. H.; Wang, S.; Bai, Y.; Wang, P. P.; Li, J. J.; Chu, Z. W.; Chen, G. H. Polyurethane foam functionalized with an AIE-active polymer using an ultrasonication-assisted method: preparation and application for the detection of explosives. *RSC Adv.* **2016**, *6*, 26950–26953.

(31) Niu, Y. Q.; He, T.; Song, J.; Chen, S. P.; Liu, X. Y.; Chen, Z. G.; Yu, Y. J.; Chen, S. G. A new AIE multi-block polyurethane copolymer material for subcellular microfilament imaging in living cells. *Chem. Commun.* **2017**, *53*, 7541–7544.

(32) Wu, Y.; Hu, J.; Huang, H.; Li, J.; Zhu, Y.; Tang, B.; Han, J.; Li, L. Memory chromic polyurethane with tetraphenylethylene. *J. Polym. Sci. Pol. Phys.* **2014**, *52*, 104–110.

(33) Sun, W.; Wang, Z.; Wang, T.; Yang, L.; Jiang, J.; Zhang, X.; Luo, Y.; Zhang, G. Protonation-Induced Room-Temperature Phosphorescence in Fluorescent Polyurethane. *J. Phys. Chem. A* **2017**, *121*, 4225–4232.

(34) Dias, F. B.; Bourdakos, K. N.; Jankus, V.; Moss, K. C.; Kamtekar, K. T.; Bhalla, V.; Santos, J.; Bryce, M. R.; Monkman, A. P. Triplet harvesting with 100% efficiency by way of thermally activated delayed fluorescence in charge transfer OLED emitters. *Adv. Mater.* **2013**, *25*, 3707–3714.

(35) Mei, J.; Hong, Y.; Lam, J. W.; Qin, A.; Tang, Y.; Tang, B. Z. Aggregation-induced emission: the whole is more brilliant than the parts. *Adv. Mater.* **2014**, *26*, 5429–5479.

(36) Wan, Q.; Liu, M.; Mao, L.; Jiang, R.; Xu, D.; Huang, H.; Dai, Y.; Deng, F.; Zhang, X.; Wei, Y. Preparation of PEGylated polymeric nanoprobes with aggregation-induced emission feature through the combination of chain transfer free radical polymerization and multicomponent reaction: Self-assembly, characterization and biological imaging applications. *Mat. Sci. Eng. C-Mater. Biol. Appl.* **2017**, *72*, 352–358.

(37) Mohamed, M. G.; Lu, F.-H.; Hong, J.-L.; Kuo, S.-W. Strong emission of 2,4, 6-triphenylpyridine-functionalized polytyrosine and hydrogen-bonding interactions with poly (4-vinylpyridine). *Poly. Chem.* **2015**, *6*, 6340–6350.

(38) Zhang, G.; Chen, J.; Payne, S. J.; Kooi, S. E.; Demas, J. N.; Fraser, C. L. Multi-emissive difluoroboron dibenzoylmethane polylactide exhibiting intense fluorescence and oxygen-sensitive room-temperature phosphorescence. *J. Am. Chem. Soc.* **2007**, *129*, 8942–8943.

(39) Zhang, G.; Palmer, G. M.; Dewhirst, M. W.; Fraser, C. L. A dual-emissive-materials design concept enables tumour hypoxia imaging. *Nat. Mater.* **2009**, *8*, 747–751.

(40) Zhang, X.; Xie, T.; Cui, M.; Yang, L.; Sun, X.; Jiang, J.; Zhang, G. General design strategy for aromatic ketone-based single component dual-emissive materials. *ACS Appl. Mater. Interfaces* **2014**, *6*, 2279−2284.

(41) Zhou, C.; Xie, T.; Zhou, R.; Trindle, C. O.; Tikman, Y.; Zhang, X.; Zhang, G. Waterborne polyurethanes with tunable fluorescence and room temperature phosphorescence. *ACS Appl. Mater. Interfaces* **2015**, *7*, 17209−17216.

(42) Chen, X.; Xu, C.;Wang, T.; Zhou, C.; Du, J.; Wang, Z.; Xu, H.; Xie, T.; Bi, G.; Jiang, J.; Zhang, X.; Demas, J. N.; Trindle, C. O.; Luo, Y.; Zhang, G. Versatile room-temperature-phosphorescent materials prepared from N-substituted naphthalimides: emission enhancement and chemical conjugation. *Angew. Chem. Int. Ed*. **2016**, *55*, 9872–9876.

(43) Zhang, G.; Evans, R. E.; Campbell, K. A.; Fraser, C. L. Role of boron in the polymer chemistry and photophysical properties of difluoroboron–dibenzoylmethane polylactide. *Macromolecules* **2009**, *42*, 8627–8633. (44) Menning, S.; Kramer, M.; Coombs, B. A.; Rominger, F.; Beeby, A.; Dreuw, A.; Bunz, U. H. Twisted tethered tolanes: Unanticipated long-lived phosphorescence at 77 K. *J. Am. Chem. Soc.* **2013**, *135*, 2160–2163.

(45) Hong, Y.; Lam, J. W. Y.; Tang, B. Z. Aggregation-induced emission: phenomenon, mechanism and applications. *Chem. Commun.* **2009**, 4332–4353.

(46) Etherington, M. K.; Gibson, J.; Higginbotham, H. F.; Penfold, T. J.; Monkman, A. P. Revealing the spin–vibronic coupling mechanism of thermally activated delayed fluorescence. *Nat. Commun.* **2016**, *7*, 13680.

(47) Congreve, D. N.; Lee, J.; Thompson, N. J.; Hontz, E.; Yost, S. R.; Reusswig, P. D.; Bahlke, M. E.; Reineke, S.; Van Voorhis, T.; Baldo, M. A. External quantum efficiency above 100% in a singlet-exciton-fission–based organic photovoltaic cell. *Science* **2013**, *340*, 334–337.

(48) Yang, Z.; Mao, Z.; Zhang, X.; Ou, D.; Mu, Y.; Zhang, Y.; Zhao, C.; Liu, S.; Chi, Z.; Xu, J.; Wu, Y. C.; Lu, P. Y.; Lien, A.; Bryce, M. R. Intermolecular Electronic Coupling of Organic Units for Efficient Persistent Room-Temperature Phosphorescence. *Angew. Chem. Int. Ed.* **2016**, *55*, 2181–2185.

(49) Xie, Y.; Ge, Y.; Peng, Q.; Li, C.; Li, Q.; Li, Z. How the Molecular Packing Affects the Room Temperature Phosphorescence in Pure Organic Compounds: Ingenious Molecular Design, Detailed Crystal Analysis, and Rational Theoretical Calculations. *Adv. Mater.* **2017**, *29*, 1606829.

(50) An, Z.; Zheng, C.; Tao, Y.; Chen, R.; Shi, H.; Chen, T.; Wang, Z.; Li, H.; Deng, R.; Liu, X.; Huang, W. Stabilizing triplet excited states for ultralong organic phosphorescence. *Nat. Mater.* **2015**, *14*, 685–690.

(51) He, Z.; Zhao, W.; Lam, J. W. Y.; Peng, Q.; Ma, H.; Liang, G.; Shuai, Z.; Tang, B. Z. White light emission from a single organic molecule with dual phosphorescence at room temperature. *Nat. Commun.* **2017**, *8*, 416.

(52) Yuan, W. Z.; Shen, X. Y.; Zhao, H.; Lam, J. W. Y.; Tang, L.; Lu, P.; Wang, C.; Liu, Y.; Wang, Z.; Zheng, Q.; Sun, J. Z.; Ma, Y.; Tang, B. Z. Crystallization-induced phosphorescence of pure organic luminogens at room temperature. *J. Phys. Chem. C* **2010**, *114*, 6090–6099.

(53) Zhao, W.; He, Z.; Lam, J. W. Y.; Peng, Q.; Ma, H.; Shuai, Z.; Bai, G.; Hao, J.; Tang, B. Z. Rational molecular design for achieving persistent and efficient pure organic room-temperature phosphorescence. *Chem* **2016**, *1*, 592–602.

(54) Li, Q.; Li, Z. The strong light-emission materials in the aggregated state: what happens from a single molecule to the collective group. *Adv. Sci.* **2017**, *4*, 1600484.

(55) Yang, J.; Ren, Z.; Xie, Z.; Liu, Y.; Wang, C.; Xie, Y.; Peng, Q.; Xu, B.; Tian, W.; Zhang, F.; Chi, Z.; Li, Q.; Li, Z. AIEgen with fluorescence–phosphorescence dual mechanoluminescence at room temperature. *Angew. Chem. Int. Ed.* **2017**, *56*, 880–884.

(56) Yang, J.; Zhen, X.; Wang, B.; Gao, X.; Ren, Z.; Wang, J.; Xie, Y.; Li, J.; Peng, Q.; Pu, K.; Li, Z. The influence of the molecular packing on the room temperature phosphorescence of purely organic luminogens. *Nat. Commun.* **2018**, *9*, 840.

Supporting Information

Aggregation-Induced Long-Lived Phosphorescence in Non-Conjugated Polyurethane Derivatives at 77 K

Nan Jiang,[†,‖] Guang-Fu Li,[†,‖] Bao-Hua Zhang,[#] Dong-Xia Zhu,*[,†] Zhong-Min Su,*[,†] and Martin R. Bryce*[,§]

[†] Key Laboratory of Nanobiosensing and Nanobioanalysis at Universities of Jilin Province, Faculty of Chemistry, Northeast Normal University, Renmin Street No. 5268, Changchun 130024, P. R. China

[#] State Key Laboratory of Polymer Physics and Chemistry, Changchun Institute of Applied Chemistry, Chinese Academy of Sciences, Changchun 130022, P. R. China

[§] Department of Chemistry, Durham University, Durham DH1 3LE, UK

Contents: **Page**

1. Experimental - general information

Materials obtained from commercial suppliers were used without further purification unless otherwise stated. All glassware, syringes, magnetic stirring bars, and needles were thoroughly dried in a convection oven. ^{1}H NMR spectra were recorded at 25 ºC on a Varian 500 MHz spectrometer. The ^{1}H NMR spectra were referenced internally to the residual proton resonance in DMSO-d_6 (δ 2.5 ppm). The molecular weights of the polymers were determined by gel permeation chromatography (GPC) on a Waters 410 instrument with monodispersed polystyrene as the reference and THF as the eluent at 35 °C. The *M*n values for all PUs were also calculated from ^{1}H NMR spectra. For **PU1** and **PU2**, the calculated values from ^{1}H NMR were consistent with the data measured from GPC to within 300 g mol^{-1}. Transmission electron microscopy (TEM) was performed using a TECNAI F20 microscope. The samples were prepared by placing microdrops of the solution on a holey carbon copper grid. UV-vis absorption spectra were recorded on a Shimadzu UV-3100 spectrophotometer. Photoluminescence spectra were collected on an Edinburgh FLS920 spectrophotometer. IR spectroscopy was conducted using KBr pellets with an Nicolet 6700 FT/IR spectrophotometer ranging from 4000 to 400 cm^{-1}. Powder X-ray diffraction (XRD) patterns of the samples were collected on a Rigaku Dmax 2000.

2. Structural characterization

To investigate the effect of the degree of polymerization on LPL, different chain length samples of **PU1** and **PU2** were also synthesized by the same synthetic route as for **PU1** and **PU2** (*M*n = 3118 and 1845 g mol^{-1}). The *M*n values for the new **PU1** and **PU2** samples were measured as 2672 g mol^{-1} 2204 g mol^{-1}, respectively, from GPC.

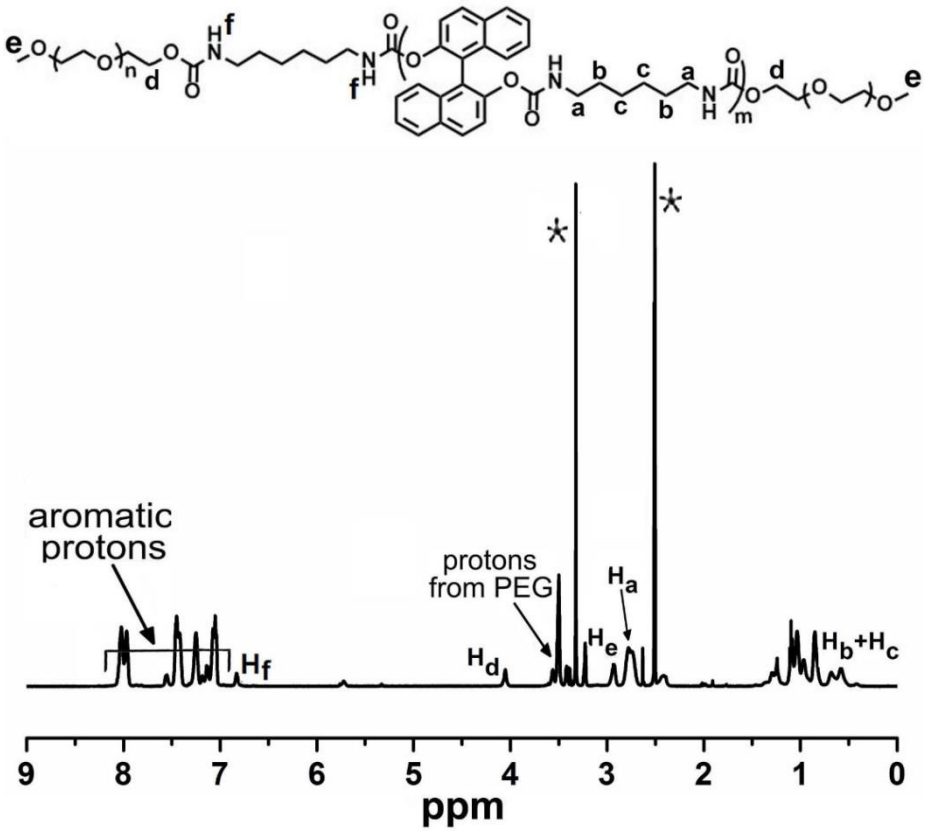

Figure S1. ^{1}H NMR spectrum of **PU1** in DMSO-d_6 (* indicates peaks from the solvent and water)

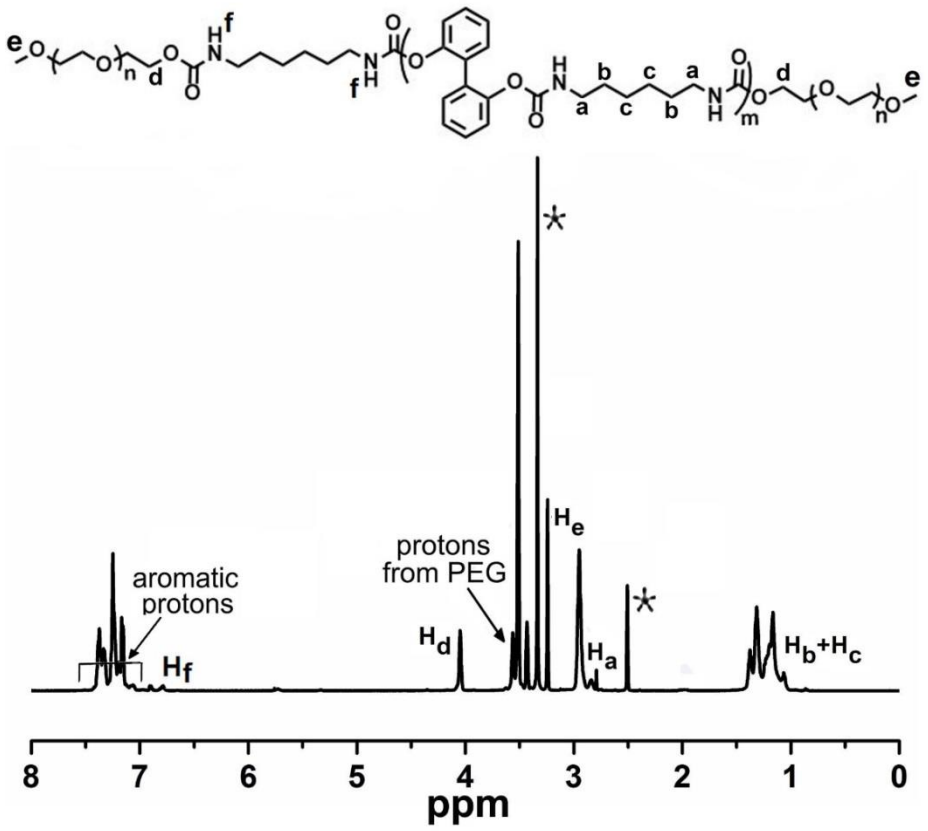

Figure S2. ^{1}H NMR spectrum of **PU2** in DMSO-d_6 (* identifies peaks from solvent and water)

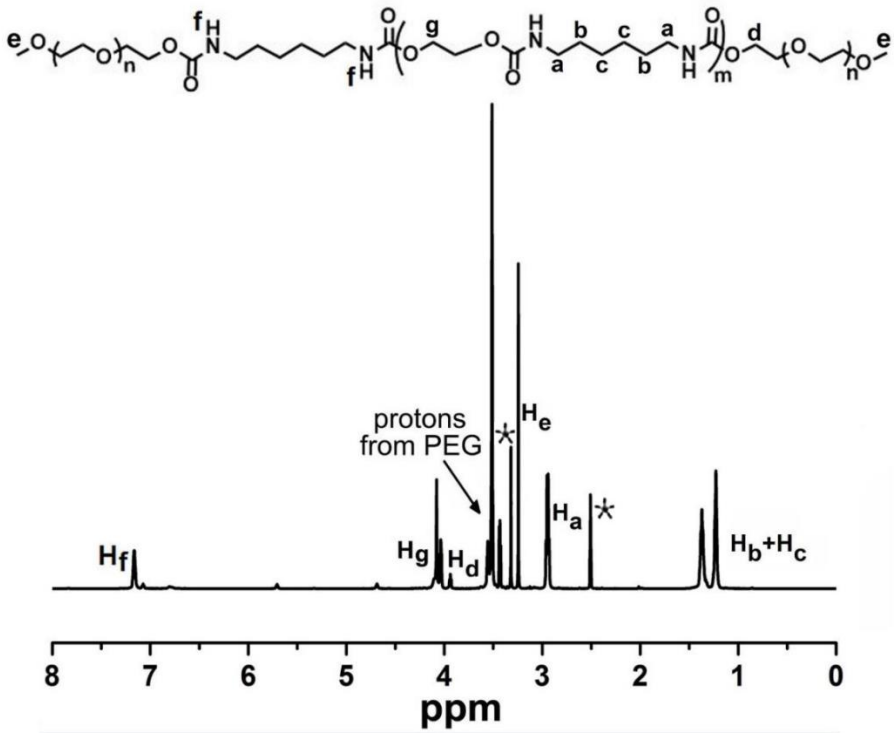

Figure S3. ^{1}H NMR spectrum of **PU3** in DMSO-d_6 (* indicates peaks from the solvent and water).

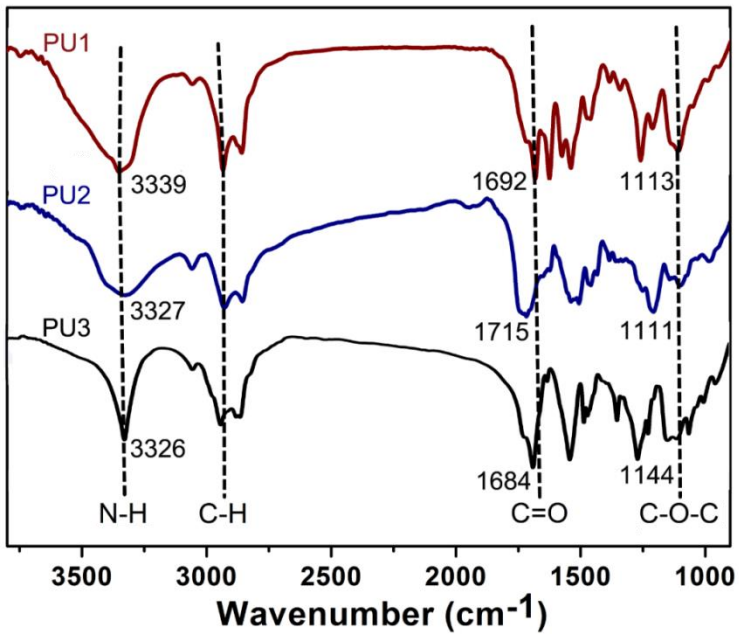

Figure S4. FTIR spectra of **PU1**, **PU2** and **PU3**.

3. Photophysical properties

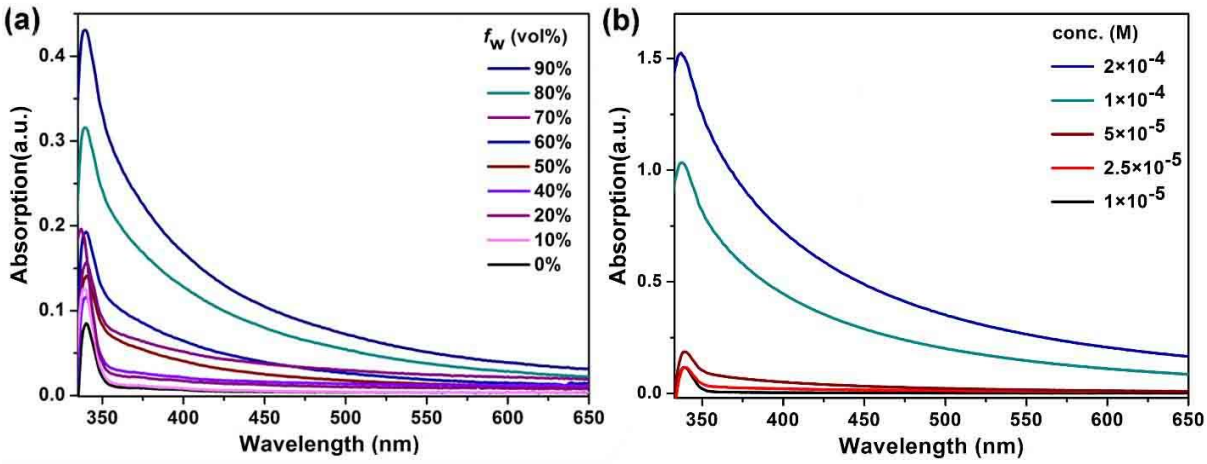

Figure S5. (a) UV-visible absorption spectra of **PU1** in acetone-water mixtures with different water fractions (0–90%, v/v) at room temperature. (b) UV-visible absorption spectra of **PU1**/acetone at different molar concentrations.

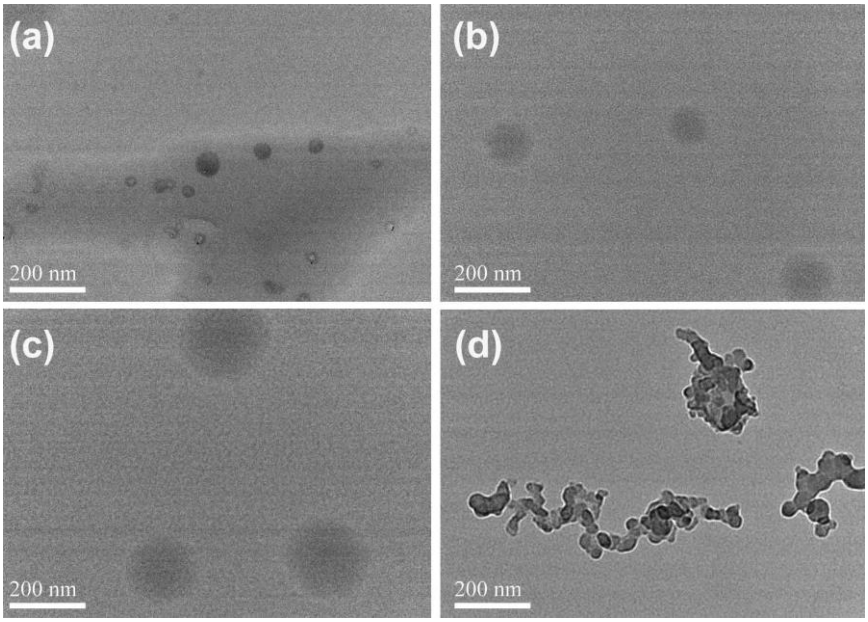

Figure S6. TEM images of nanoaggregates of **PU1** formed in (a) acetone solution (10^{-5} M), (b) acetone solution (10^{-4} M), (c) acetone solution (2×10^{-4} M) and (d) acetone–H_2O mixtures with 90% water fraction (10^{-5} M).

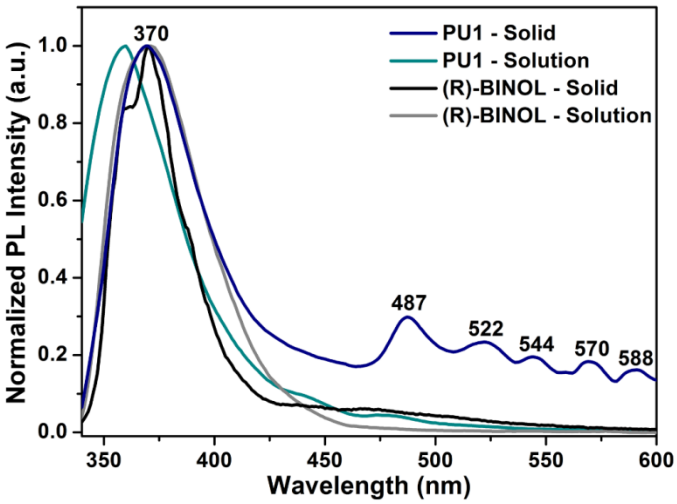

Figure S7. PL spectra of monomer (*R*)-BINOL (black lines) and **PU1** (blue lines) at room temperature.

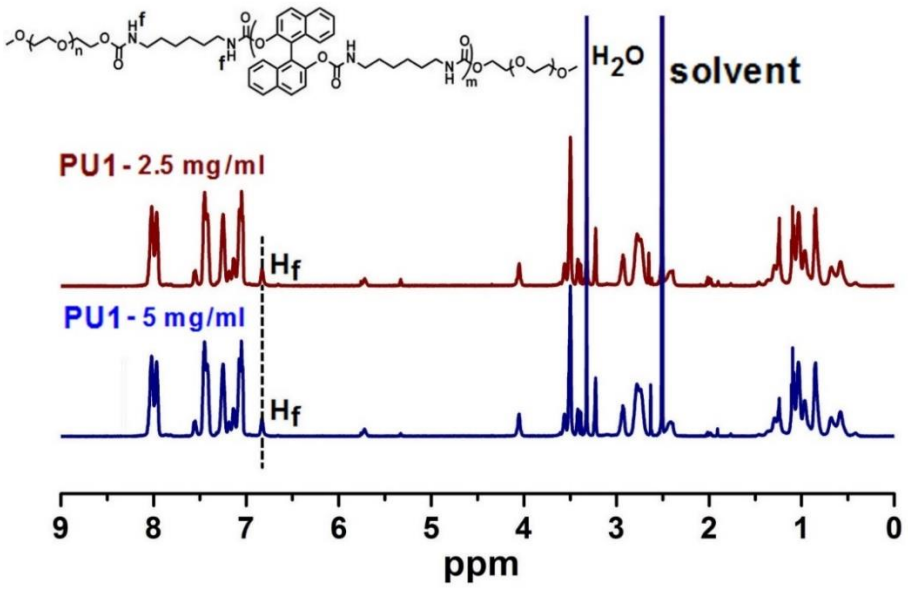

Figure S8. ^{1}H NMR spectra of **PU1**-2.5 mg/mL and **PU1**-5 mg/mL in DMSO-d_6.

3. Photophysical Properties

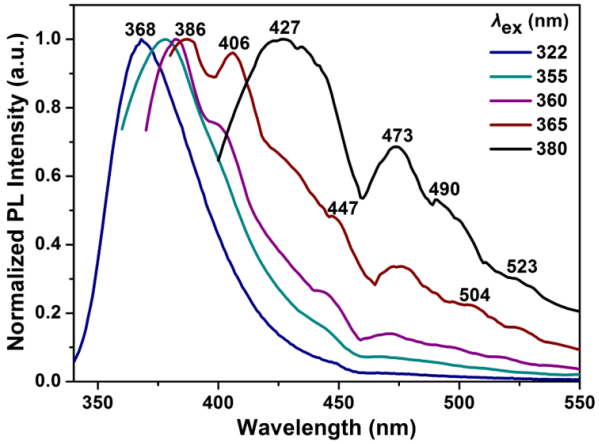

Figure S9. Steady-state PL spectra of **PU1** in powder state with varying λ_{ex}.

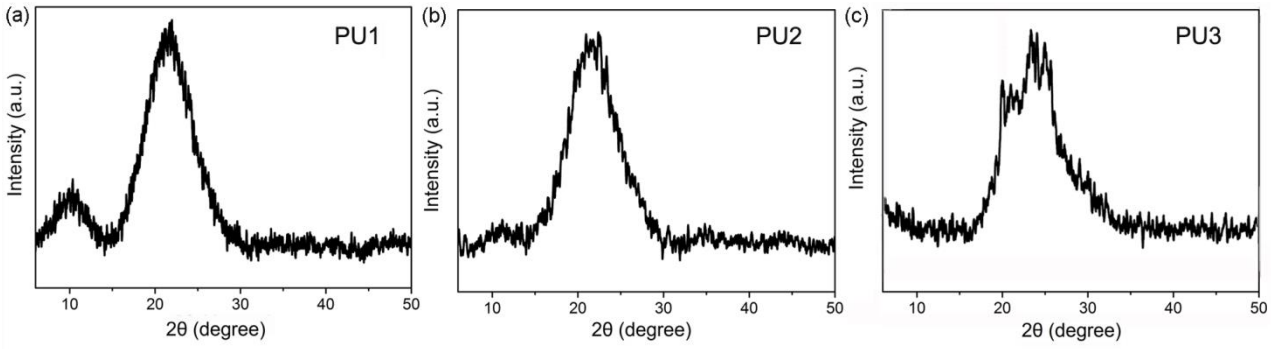

Figure S10. Powder XRD patterns of **PU1, PU2** and **PU3**.

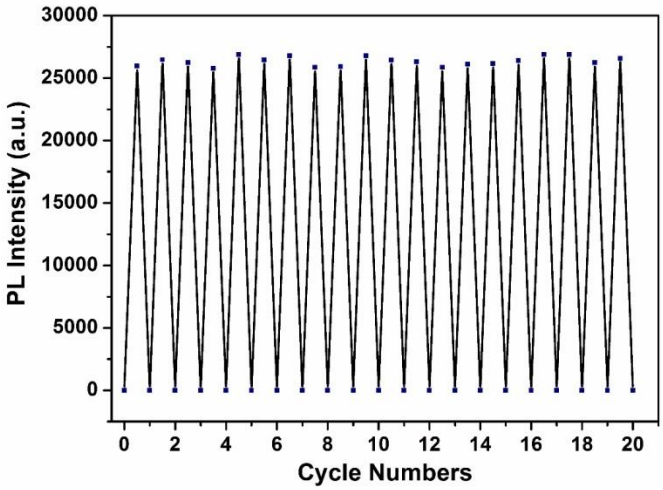

Figure S11. The repeated intensity scans of **PU1** for 20 cycles without photo-bleaching.

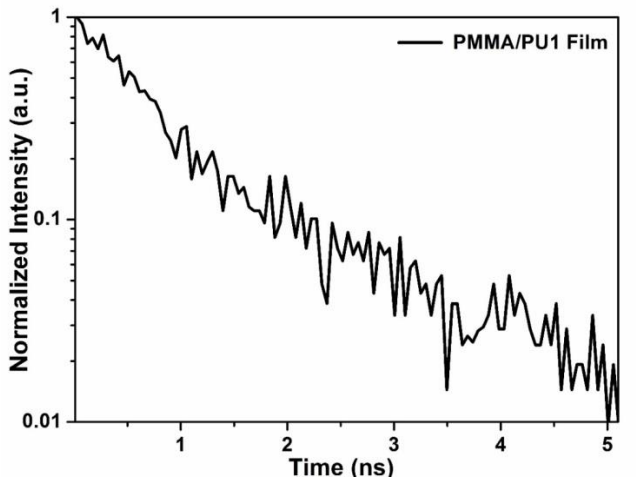

Figure S12. Emission decay of **PU1** in PMMA doped film state (2 wt. % of **PU1**) at 77 K.

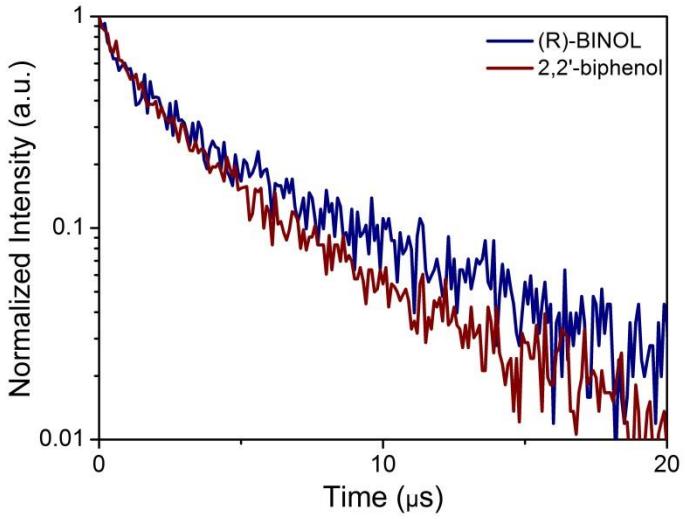

Figure S13. Phosphorescence decays at 550 nm of (R)-BINOL and 2,2'-biphenol in 2-MeTHF solution at 77 K.

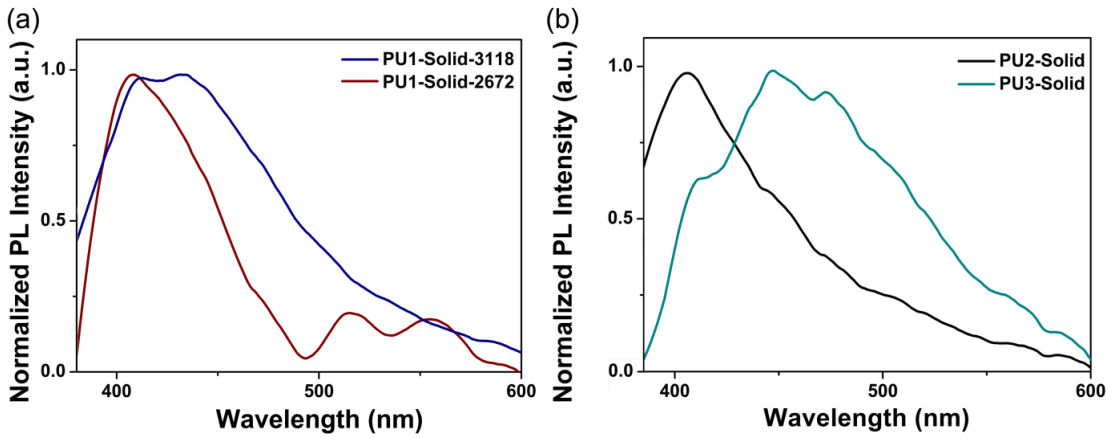

Figure S14. (a) Steady-state PL spectra of **PU1** in powder state with two different M_n values (3118 and 2672 g mol $^{-1}$) at 77 K. (b) Steady-state PL spectra of **PU2** and **PU3** in powder state at 77 K.

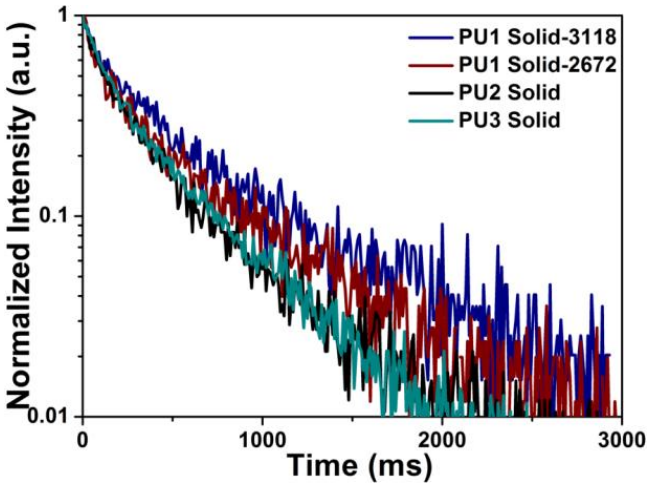

Figure S15. Phosphorescence decays at 550 nm of **PU1**-**PU3** in powder state. Data for **PU1** are for samples with M_n values 3118 and 2672 g mol $^{-1}$.

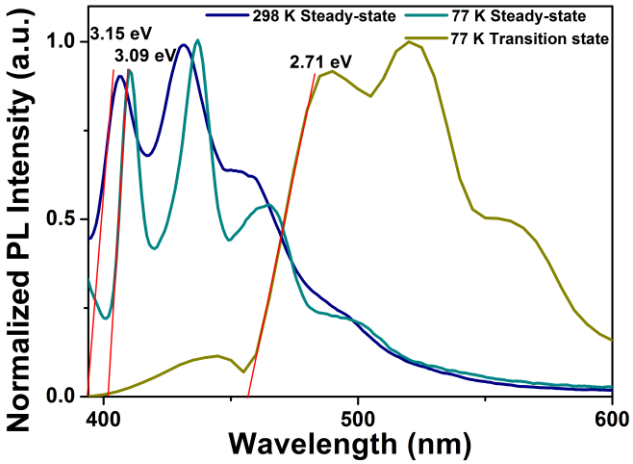

Figure S16. Steady-state and transition-state emission spectra in the solution state and corresponding excited energy levels of S_1, T_1 and T_1^* states of **PU1** with M_n 3118 g mol^{-1}.

Table S1. The phosphorescent decays of **PU1** in 2-methyltetrahydrofuran solution with different concentrations at 77 K

		495 nm	**525 nm**	**560 nm**	
10^{-2} M	**M_n = 3118**	1083.68 ms	1147.95 ms	1437.91 ms	
	M_n = 2672	948.66 ms	972.14 ms	1083.68 ms	
		445 nm	**490 nm**	**513 nm**	**560 nm**
10^{-5} M	**M_n = 3118**	762.85 ms	799.76 ms	829.54 ms	762.57 ms
	M_n = 2672	607.99 ms	749.70 ms	757.39 ms	615.29 ms

Table S2. The phosphorescent decays of **PU1–PU3** in powder state at 77 K

		520 nm	**550 nm**
PU1	**M_n = 3118 g mol^{-1}**	463.76 ms	518.60 ms
	M_n = 2672 g mol^{-1}	355.58 ms	437.60 ms
PU2		**450 nm**	**494 nm**
	M_n = 2204 g mol^{-1}	322.51 ms	546.58 ms
	M_n = 1845 g mol^{-1}	392.72 ms	410.09 ms
PU3		**497 nm**	**525 nm**
	M_n = 3544 g mol^{-1}	295.59 ms	323.26 ms

Table S3. The phosphorescent decays of **PU1** in pristine film state at 77 K

		535 nm	**545 nm**
PU1	**10 mg**	319.53 ms	364.81 ms
(M_n = 2672 g mol^{-1})	**100 mg**	426.67 ms	413.05 ms